e-ISSN: 2582-5208
International Research Journal of Modernization in Engineering Technology and Science
(Peer-Reviewed, Open Access, Fully Refereed International Journal)
Volume:03/Issue:09/September-2021 Impact Factor- 6.752 www.irjmets.com

OPTIMAL PEROVSKITE SOLAR CELL PERFORMANCE BASED ON SOLAR CONCENTRATION POWER USING A TRACKING SYSTEM AND FUZZY CONTROL SYSTEM

Shivani Vashishtha[*1], Prof. Vishal Sharma[*2], Dr. Shubhendra Pratap Singh[*3]

[*1,3]Department Of Electrical Engineering, Roorkee Institute Of Technology, Roorkee Uttrakhand-247667, India.

[*2]ECE/EEE/EE Department, School Of Technology, Roorkee Institute Of Technology, Roorkee Uttrakhand-247667, India.

ABSTRACT

This study provides an actual experimental technique with an innovative tracking method for a solar concentrator in order to increase the solar power to a large level and also provides a flawless, functional control system for length available solar power. The theoretical value should be approximately 50% larger if merely a solar panel is used. The method is arranged utilizing Solar Tracker and Double Sun Technology. This method results in a significant boost in output power, the output power rises by 68.45 percent by using a solar tracking panel with four flat reflectors. The test is carried out in four different configurations. In first installation, the power production is determined using a dual solar tracker. Power is measured using Double Sun in second setup. In the third setup, solar tracker and Double Sun are employed. In addition to the tracker, four flat reflectors are also included. Finally, using fuzzy logic, the suggested system optimizes total output by maximizing the amount of photovoltaic energy used and the period of time that solar energy is accessible. For computer developed iodide methylammonium lead (CH3NH3PbI3, perovskite solar cell, we have investigated how sun concentration affects PV performance. The functional density theory (DFT) will be employed in calculating, band structure, band gap, and states density (DOS) of CH3NH3PbI3. Through this method of balance is used to determine the influence of concentration of perovskite solar cell performance.

Keywords: Solar Tracker, Double Sun Technology, Concentrator, Passive Device Fuzzy Logic, Photovoltaic (PV) Panel, Band Structure, Band Gap.

I. INTRODUCTION

In the twenty-first century, power generation will take on a completely new shape. Coal, gas, and petroleum are all fossil fuels that will be in short supply for generation of energy. Renewable energy is a superior alternate to fossil fuels since it has a lower environmental impact. Though hydroelectricity has the potential to provide a large It is not available in all parts of the globe. As an alternative, solar energy can be used to generate electricity, has every chance of replacing the current power producing system. [1]. Using solar energy is possible in very small industries and large sectors, such as clothing companies that use solar energy as Lighting and ventilation from a backup power source. However, photovoltaic (PV) panels have a low output power [2]. According to extensive research, One of two approaches can be used to increase the output power, manufacturing or passive devices. [3-7]. Therefore, passive devices are expensive and difficult to manufacture, both the efficiency and the filling factor are commonly used. To increase the amount of solar power, concentrators with two flat mirrors and a solar tracker are utilized. The double sun technology is known as the concentration with two flat mirrors.

The global average rate of energy use is increasing. A daily solar radiation incidence at sea level of around 2 x1017 W was determined to be around 12,500 times as high as the global average in 2006 [8]. The global climate is greatly impaired with the increased use of conventional energy. The abundance of solar energy does not do harm to the ecosystem. Solar cells are the most efficient way to harness the sun's energy. Solar cells are being studied by scientists who are attempting to improve their efficiency by experimenting with various materials. Solar cell efficiency for perovskite materials have increased from 3.8 percent in 2009 [9] to 23.3 percent in late 2018 [10-11]. Perovskite solar cells made of methylammonium lead triiodide (CH3NH3PbI3)

e-ISSN: 2582-5208
International Research Journal of Modernization in Engineering Technology and Science
(Peer-Reviewed, Open Access, Fully Refereed International Journal)
Volume:03/Issue:09/September-2021 Impact Factor- 6.752 www.irjmets.com

offer unique properties Direct bandgap, light weight, thinness, and flexibility, inexpensive raw material and fabrication costs, high absorption coefficient, and high efficiency are some of the benefits. [12-16].

Global climate and a growing need for energy call for an immense increase in the number of renewables worldwide. All photovoltaic systems (PV) have more installed capacity than all other renewable energy systems combined, which totaled 105.20 GW in 2018 and 130 GW in 2020. [17]. The sun radiation density varies from place to place. There are many strategies to stimulate the use of solar energy, including through monitoring of sun-folding solar systems. Tracking systems have as a major goal a greater energy yield, which according to earlier studies and surveys can vary between 30% and 60% compared with a fixed solar system. The drive mechanism, the freedom level, control system and other elements, such as weather or location, depend on it. Photovoltaic systems generate electricity mostly based on the amount of solar energy that hits the photovoltaic modules as well as the materials employed [18], temperature and other parameters. [19]

The effect of solar module temperature on conversion efficiency [20-21], as well as the kinds and use of photovoltaic modules [22]. Other elements effecting photovoltaic modules include the technology and other aspects, solar energy conversion efficiency is largely governed by the adaptation of impedance known as maximum power point monitoring (MPPT). The MPPT algorithm is also incredibly useful for optimizing electrical parameters to produce Optimum solar system electrical power generation. Thanks to photovoltaic monitoring devices that observe the courses of sunbeams, the energy density of solar radiation depends on the norm of the module surface. The tracking system drive assembly is controlled and used properly to achieve tracking. As the sun's energy is received directly on the modules, they are then divided according to the number of degrees of freedom (DOF). Single-axis and dual-axis [23-24] photovoltaic tracking systems are the most popular. Photovoltaic systems with a single axis trace the path of the sun by moving from East to West around an axis, while photovoltaic two-axis photovoltaic system can travel from East to West from North to South. Due to the addition of this rotating axis, however, Solar cells with two-axis tracking are more accurate than those with a single axis. Solar tracking system with dual-axis photovoltaic tracking's may not be economical otherwise, as compared to a single-axis tracking system.

II. EXPERIMENTAL SETUP

Data was obtained for three days in four distinct settings a tracking system and concentration methods to validate the energy enhancement. From 8:30 a.m. to 5:00 p.m., various current and voltage on open circuit and short circuit currents are recorded every half hour for nine hours, and power is estimated from the data. When the sun rays are at a straight angle to the solar panel surface, the most power is produced. Sun beams can be angled at the solar panel surface using fuzzy control for the duration of our chosen period. Fig. 1 A mirror-integrated solar PV system's system efficiency and utilization factor. In Fig. 2, you can see the same days' power versus time plots.

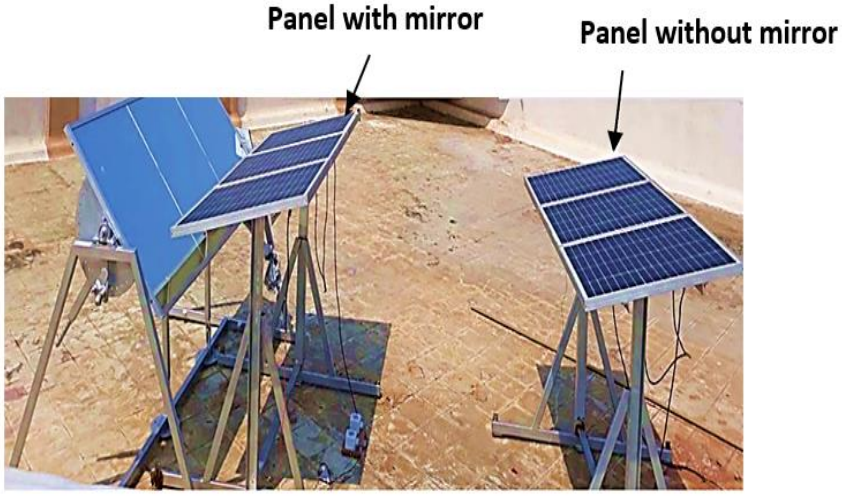

Fig 1: A mirror-integrated solar PV system's system efficiency and utilization factor

e-ISSN: 2582-5208
International Research Journal of Modernization in Engineering Technology and Science
(Peer-Reviewed, Open Access, Fully Refereed International Journal)
Volume:03/Issue:09/September-2021 Impact Factor- 6.752 www.irjmets.com

2.1 Analysis of Data

For each situation, the average output power is shown in Table 1, whereas Figure 8 displays average output power over time for each scenario. It was found that a flat PV panel set in place produced an average output power of 20.10 watts (W). Fig.3 shows the photovoltaic system. As a result of the tracking system and concentration procedures, data was collected over a period of three days in four different settings to test the energy enhancement theory. Every half hour from 8:30 am to 5:00 pm for seven hours, open circuit and short circuit currents are monitored, as indicated in table 1. There was an increase in average power output with dual sun but no tracking, in the first scenario by about 15.32 per cent. Double Sun and solar tracker have resulted in an average power output increase of 35.70 percent. Using Four Sun Technology and a solar tracker, the average output power of the system was significantly enhanced, by 60.20 percent over the initial condition, resulting in an average power of 30.45 W. Fig. 2 shows the comparision of four experimental setups with average power output

Table I: Four Experimental Setups With Average Power Output

Time (Hour)	AVERAGE OUTPUT OF POWER			
	With 4 Sun and solar tracker	**without solar tracker and concentrators and**	**With Double Sun without solar tracker**	**With Double Sun and with solar tracker**
8:30 AM	24.80	12.16	15.61	20.44
9:00 AM	27.38	13.00	16.29	21.69
9:30 AM	27.60	14.59	17.53	21.87
10:00 AM	27.91	16.20	18.41	23.18
10:30 AM	28.45	19.05	21.80	23.70
11:00 AM	28.14	20.11	22.45	24.56
11:30 AM	29.25	20.18	22.99	24.55
12:00 PM	28.46	20.90	22.98	23.18
12:30 PM	27.58	19.79	22.27	23.03
1:00 PM	27.83	19.20	21.97	23.60
1:30 PM	25.79	18.43	20.30	22.83
2:00 PM	25.49	17.26	17.83	22.67
2:30 PM	25.10	16.22	15.64	22.38
3:00 PM	25.43	14.81	15.17	22.36
3:30 PM	24.38	13.02	14.63	20.29
4:00 PM	23.45	12.02	13.23	19.22
4:30 PM	22.86	11.80	12.85	18.11
5:00 PM	21.10	10.56	11.32	17.19
Pavg	26.90	16.99	19.05	22.68
Percent Increase	61.54%	Base	4.82%	37.65%

e-ISSN: 2582-5208
International Research Journal of Modernization in Engineering Technology and Science
(Peer-Reviewed, Open Access, Fully Refereed International Journal)
Volume:03/Issue:09/September-2021 Impact Factor- 6.752 www.irjmets.com

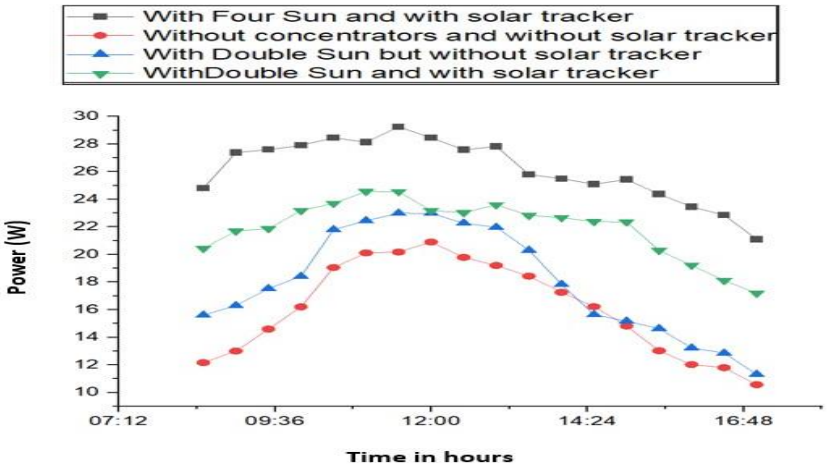

Fig 2: Comparision Four Experimental Setups With Average Power Output

III. FOUR SUN AND DOUBLE SUN TECHNOLOGY

The concentration factor is used to describe the amount of radiation that falls on the modules in this system, shows in fig. 3 The geometric concentration factor (C) is the most commonly used definition, and it is determined for this system by the ratio of the effective area (the area seen by the sun) to the active cell area, as specified by the equation 1. [8], [11]:

$$C = \frac{A_{eff}}{A_{module}} = \frac{A_{mirrors} + A_{module}}{A_{module}} = 1 + \frac{A_{mirrors}}{A_{module}} \quad (1)$$

Here, the effective area is denoted by Aeff (area that is visible to the sun), The mirror area visible to the sun is referred to as Amirrors and the module's overall area is called Amodule. Double Sun Technology was employed in this experiment

$$A_{module} = (15 \times 20.5)\ sq.inch = 307.5\ sq.inch \quad (2)$$

$$A_{mirrors} = 2 \times (10 \times 25.2)\ sq.inch = 504\ sq.inch \quad (3)$$

$$C = 2.0x \quad (4)$$

Thus, in this study, Four Sun Technology is named four flat mirrors later. Reflective losses and direct radiation are not taken into account. The theoretical model proposed by Reis took these elements into account [12].

$A_{mirrors} = 2 \times (10 \times 14 + 15 \times 20.5) sq.inch = 895\ sq.inch$

$$A_{module} = \quad (5)$$

$$(15 \times 20.5) sq.inch = 307.5\ sq.inch \quad (6)$$

$$C = 4.02x \quad (7)$$

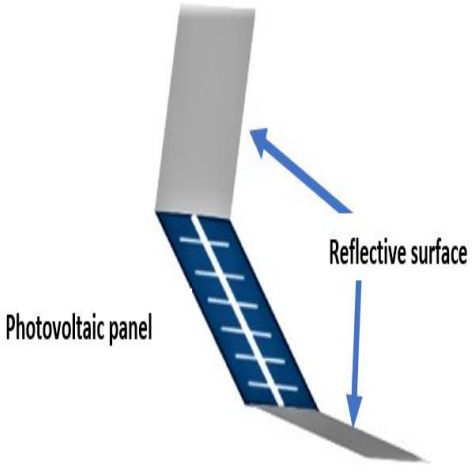

Fig 3: Photovoltaic system

e-ISSN: 2582-5208
International Research Journal of Modernization in Engineering Technology and Science
(Peer-Reviewed, Open Access, Fully Refereed International Journal)
Volume:03/Issue:09/September-2021 Impact Factor- 6.752 www.irjmets.com

IV. IMPLEMENTATION OF FUZZY LOGIC

- Structure of Fuzzy Logic Controller - As a feedback, our developed monitor uses a range of alterations to measure the light strength received from the sensor. Fig. 4 shows the underlying structure of the fuzzy control system.
- Development- The entire fuzzy controller may be designed in five phases in our suggested control system.
- Interpretation: The input, output and language variables are defined.
- The variable input is the error e.
- The number of seconds between the stepper engine rotation and correction in the reversal variable is the output, utilize Domain scope for both the output and input variables domains is determined using a normalized discrete domain.
- We can identify five linguistic terms for each language variable for linguistic items, i.e. e = NB, NS, ZE, PS, PB

  Where, PB: Positive Big, ZE: Zero, PS: Positive Small, NS: Negative Small, NB: Negative Big

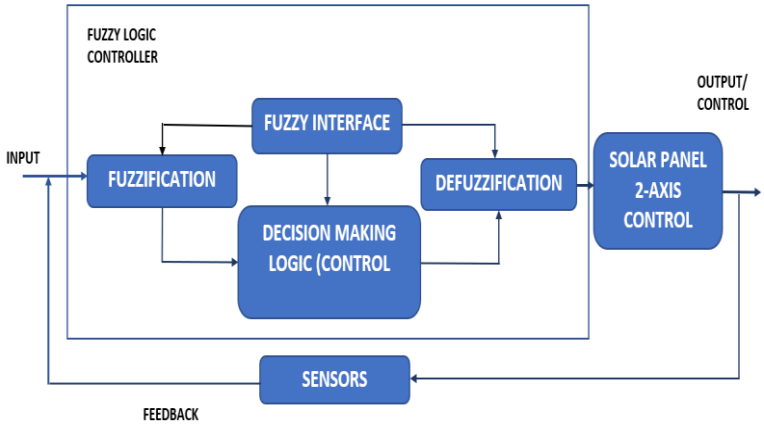

Fig 4: Structure of a Solar Energy Fuzzy Control System

- According to the provided variables, we can create membership input functions
- Base of Fuzzy Rules: Because all States must act according to the rules put down in the rule's foundation, the establishment of the fuzzy rules base is critical. For five languages, we'll use five fluent control rules with IF THEN expressions, components in order to seamlessly create a fuzzy rule base.
- As a result, there exist several fuzzy inference methods that each produce different outcomes which define Fuzzy Inference Engine
- As a defuzzification tool, we use Mamdani's suggested center of gravity technique. in our proposed control system since it is simple and reliable.

V. SIMULATION MODEL

5.1 Analysis of Data

To figure out how efficient solar cells are, PV experts use a variety of models. In this investigation, the best feasible efficiency for the organometal lead iodide- CH3NH3PbI3 was calculated using the Shockley Queisser model [11]. Following is a list of SQ model assumptions-

- The sun and solar cell temperatures are 5900 K and 390 K, separately.
- In the interband transition, there is no overlapping.
- Infinite mobility carriers are taken from VB or CB, and there must be radiative recombination between the two bands.

Solar cells with a single gap have a current-voltage characteristic given by

$$I(V) = q[Xf_s\varphi + (f_c - Xf_s)\varphi(E_g, \infty, T_c, 0) - f_c\varphi(E_g, \infty, T_c, qV \quad (8)$$

e-ISSN: 2582-5208
International Research Journal of Modernization in Engineering Technology and Science
(Peer-Reviewed, Open Access, Fully Refereed International Journal)
Volume:03/Issue:09/September-2021 Impact Factor- 6.752 www.irjmets.com

Where energy is indicated by E, X is the denotation of solar concentration, Ts and Tc denote sun and solar cell temperatures, and fs and fc Geometrical variables of the sun and solar cells are indicated. The photon flux expression [13] represents optimum cell behavior.

$$\varphi(E_1, E_h, \mu, T) = \frac{2\pi}{h^3c^2}\int_{E_1}^{E_h}\frac{E^2}{exp(E-\mu|kT)-1}dE \qquad (9)$$

where h is Planck's constant, C is chemical potential, k is Boltzmann's constant, is light speed. The PCE (power conversion efficiency) is determined.

$$PCE = \frac{V.I(V)}{X.P_{in}} \qquad (10)$$

Where Pin is given by

$$P_{in} = q\int_0^{\infty} E\,(2\pi q^3|h^3c^3)\frac{E^2}{exp(E|kT)-1}dE \qquad (11)$$

Using this equation, we determined the PCE for the solar cell CH3NH3PbI3.

5.2 DFT Calculation

DFT is an estimated answer for many bodies systems computer technology in the Schrodinger equation. DFT is used to investigate the molecules' magnetic, structural, and electronic characteristics and flaws. In the DFT approach, the density of electrons is used to measure one part of energy and a wave function is used to determine another part of energy. A squared wave function divided by the number of electrons gives us the whole electron density. according to Hohenburg-Kohn, are determined by its density. The density functional of a large number of electrons is the total ground state energy in this example. [14-15].

VI. RESULTS AND DISCUSSION

6.1 Band Gap

Software simulation Quantum Espresso is used to calculate CH3NH3PbI3 band spacing. To characterize the exchange correlation functional, we used the so-called Generalized gradient approximation (GGA). Figures 5 respectively depict the schematic graph of unit-cellular band structures [16-17]. For symmetric phase material CH3NH3PbI3 at ambient temperature the lattice constants for PM are a= 7.236 Å, b= 8.254 Å and c = 7.124 Å for monoclinic phase. The predicted methylammonium plum bandgap (CH3NH3PbI3) is 1.65eV, in other investigations, the value of the supplied experimental bandgap may differ.

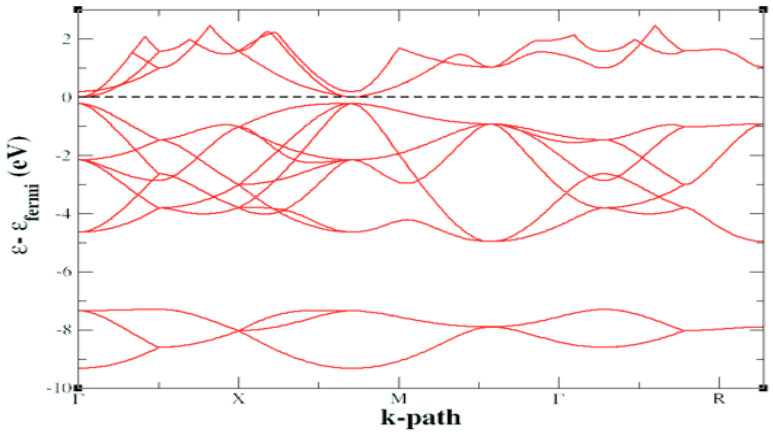

Fig 5: Methylammonium lead iodide (CH3NH3PbI3) bandgap and band structure

6.2 Comprehensive Balance Analysis

To balance the solar cell, the AM 1.2 D and AM 1.2 G solar spectrums are used. The spectrum of light that illuminates a solar cell determines its response. As a blackbody with a temperature of 6020K, the sun is often shown in artwork. Sun's temperature changes around solar disc, and light from sun is lowered by solar atmosphere, it's a little more complicated. the blackbody approximation may be called into doubt. Sun cell performance is measured using the AM 1.2 solar spectrum, which takes into account the earth's atmospheric

e-ISSN: 2582-5208
International Research Journal of Modernization in Engineering Technology and Science
(Peer-Reviewed, Open Access, Fully Refereed International Journal)
Volume:03/Issue:09/September-2021 Impact Factor- 6.752 www.irjmets.com

conditions. These effects are amplified by the atmosphere's longer optical path lengths. The photovoltaic community uses these wavelengths for solar cells.[18].

Fig. 6. Depicts the I-V properties of a single-gap perovskite,while the Fig. 7 Solar cell I-V features performed for predicted bandgap at varying Dotted lines indicate results of 1.2 G and 1.2 D, respectively, while solid lines reflect results of solar concentration

A photovoltaic cell's performance is depicted at various sunlight concentrations (from 1 sun = no concentration to 46,198 sun = full concentration). Figures 5 show the detailed balance performance of the CH3NH3PbI3 solar cell for the measured bandgap (Eg = 1.2 eV) and estimated bandgap (Eg = 1.45 eV), respectively.

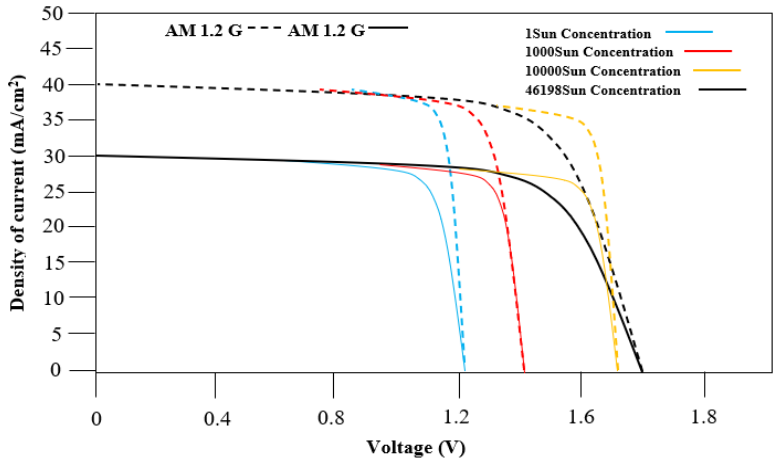

Fig 6: The I-V properties of a single-gap perovskite, CH3NH3PbI3) Air Mass 1.2 G and 1.2 D are indicated by dotted and solid lines respectively.

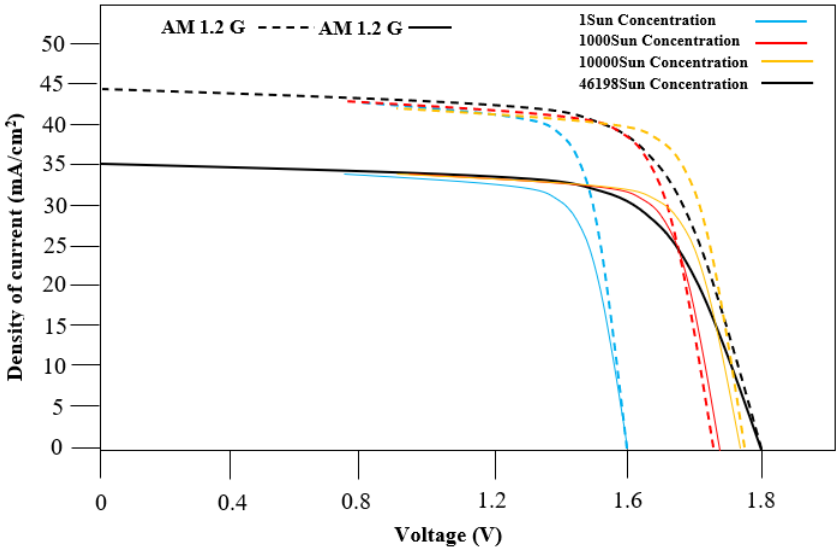

Fig 7: Solar cell I-V features performed for predicted bandgap at varying Dotted lines indicate results of 1.2 G and 1.2 D, respectively, while solid lines reflect results of solar concentration

Table II: Experiment With Bandgap At Various Solar Concentrations.

Spectrum	Efficiency			
	1 sun	1000 sun	10000 sun	46198 sun
AM 1.2 G	40.02	39.02	38.85	39.10
AM 1.2 D	29.26	29.36	28.21	30.22

e-ISSN: 2582-5208
International Research Journal of Modernization in Engineering Technology and Science
(Peer-Reviewed, Open Access, Fully Refereed International Journal)
Volume:03/Issue:09/September-2021 Impact Factor- 6.752 www.irjmets.com

Table III: Efficiency For Methylammoniology

Spectrum	Efficiency			
	1 sun	1000 sun	10000 sun	46198 sun
AM 1.2 G	45.01	44.02	43.25	44.85
AM 1.2 D	35.26	34.20	33.40	34.10

A number of I-V features. The experimental band gap permits larger current (Isc) of the short circuit compared to the calculated band gap because the value of the experimental band gap takes a greater percentage of the solar spectrum. But the experimental bandgap establishes a basic restriction on the open circuit voltage.

In table 1 and table 2, the power conversion efficiency in the varied sun concentrations of this methylemmonium lead iodide solar cell is given for both AM 1.2 G and AM 1.2 D. The efficiencies for experimental and computed band gaps are displayed in the Fig. 8 and Fig. 9 accordingly for various sun concentrations. All statistics are based on a thorough balance efficiency of 1 solar concentration to 46,198 suns (full concentration).

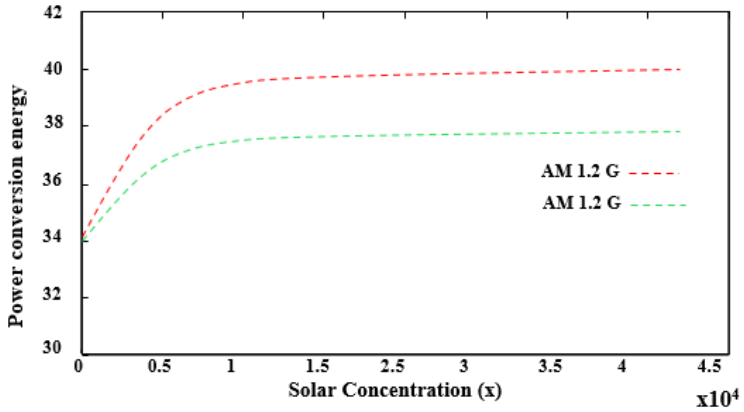

Fig 8: Single-gap perovskites (CH3NH3PbI3), A single-gap power converter's power conversion efficiency (PCE), AM 1.2 G and AM 1.2 D, both experimentally bandgap solar cell with varied sun concentration.

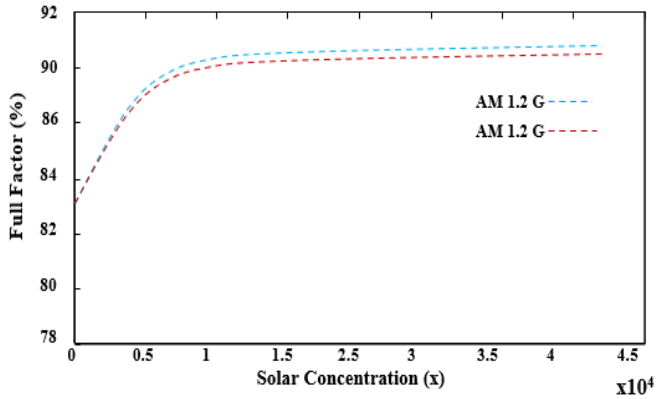

Fig 9: Filled factor of for both 1.2 G AM and 1.2 D, the solar cell with variable sun concentration at a specified bandgap

The efficiency of the solar cell grows with the maximum concentration in solar cell energy. For the experimental band gap (e = 1.2 eV), the maximum efficiency achieved is 40.20 percent for AM 1.2G and 41.22 percent for AM 1.2 The maximum efficiency has been found in AM 1.2G (eg = 1.90 eV), for AM 1.5G (40.20%) and AM 1.2 D (41.22%). Figures 8 and 9 show the fill factors at various sun concentrations for the experimental and calculated bandgaps, respectively. In varying concentrations, the AM 1.2 G and AM 1.2 D yield almost the same fill factor values

The experimental fill factors were evaluated, and the bandgap was calculated as a function of solar concentration. Fills are not at all 74.65%, 76.50% for experimental and computed band gap at AM 1.2 G correspondingly. Fill factors are 74.65 percent at no concentration, 78.40 percent at AM 1.2 D at both experimental and computed bandgap. For the experimental and computed bandgap, 90.50% and 91.50% of the full concentration fill factors for AM 1.2 G correspondingly are. For the AM 1.2 D bandgap, both experimental and calculated bandgaps were used., There are 92.37 and 93.50 percent filling factors under the full concentration range. Increased filling factors increase cell performance. Solar cells contain methylammonium lead iodide (CCH3NH3PbI3) with high solar spectra fill factors. With rising sun concentration, the filling factors are enhanced.

VII. CONCLUSION

This research demonstrated the test findings of the performance of the double solar and four solar-centered PV systems employing ordinary silicone modules and no active cooling containing geometrical concentration parameters of 2.0x and 4.02x, respectively. With solar tracker, the results of the Double Sun technology are up 33.0%. It shows also Four flat mirrors and a solar tracker can be used to increase the efficiency of solar panels boost average output power by 60.21 percent. This research also developed control system with fuzzy logic to increase overall output by maximizing the photovoltaic output available and maximizing the length of time available for solar power. The proposed sun-tracking and fumigation controller Four Sun approach is a simple and cost-efficient way to increase solar panel energy.

In this work, we tested the effect on various cell performance parameters of sun concentration. Calculation of the bandgap of iodide perovskite in methylammonium lead by means of DFT. For the efficiency calculation of CH3NH3PbI3 solar cell, a detailed balance approach is applied.. In this work, we tested the effect on various cell performance parameters of sun concentration. For the efficiency calculation of CH3NH3PbI3 solar cell, a detailed balance approach is applied. We conducted our research in both AM 1.2 D and AM 1.2 G.

VIII. REFERENCES

[1] Kreith and D. Y. Goswami, Handbook of Energy Efficiency and Renewable Energy. CRC Press, Taylor & Francis Group, 2007.

[2] A. McEvoy, T. Markvart, and L. Castaner, Practical Handbook of Photovoltaic: Fundamentals and Applications. Academic Press, 2011.

[3] M. Brogren, “Optical efficiency of low-concentrating solar energy sys- tems with parabolic reflectors,” Doctoral thesis, 2004.

[4] R. M. Swanson, “The promise of concentrators,” Progress in Photo- voltaics: Research and Applications, vol. 8, no. 1, pp. 93–111, 2000.

[5] A. Luque and S. Hegedus, Handbook of Photovoltaic Science and Engineering. John Wiley & Sons, 2011.

[6] R. B. Pettit and E. P. Roth, Solar Mirror Materials: Their Properties and Uses in Solar Concentrating Collectors. Solar Materials Science, 1980.

[7] A. Luque, G. Sala, and I. L. Heredia, “Photovoltaic concentration at the onset of its commercial deployment,” Progress in Photovoltaics: Research and Applications, vol. 14, no. 5, pp. 413–428, 2006.

[8] Twidell, J. and Weir, T. (n.d.). Renewable energy resources.

[9] A. Kojima, K. Teshima, Y. Shirai and T. Miyasaka, "Organometal Halide Perovskites as Visible-Light Sensitizers for Photovoltaic Cells", Journal of the American Chemical Society, vol. 131, no. 17, pp. 6050-6051, 2009.

[10] Djurišić, A., Liu, F., Tam, H., Wong, M., Ng, A., Surya, C., Chen, W. and He, Z. (2017). Perovskite solar cells - An overview of critical issues. Progress in Quantum Electronics, 53, pp.1-37.

[11] "National Renewable Energy Laboratory (NREL) Home Page | NREL", Nrel.gov, 2018.

[12] G. Hodes, "Perovskite-Based Solar Cells", Science, vol. 342, no. 6156, pp. 317-318, 2013.

[13] M. Green, A. Ho-Baillie and H. Snaith, "The emergence of perovskite solar cells", Nature Photonics, vol. 8, no. 7, pp. 506-514, 2014.

e-ISSN: 2582-5208
International Research Journal of Modernization in Engineering Technology and Science
(Peer-Reviewed, Open Access, Fully Refereed International Journal)
Volume:03/Issue:09/September-2021 Impact Factor- 6.752 www.irjmets.com

[14] P. Gao, M. Grätzel and M. Nazeeruddin, "Organohalide lead perovskites for photovoltaic applications", Energy Environ. Sci., vol. 7, no. 8, pp. 2448-2463, 2014.

[15] H. Snaith et al., "Anomalous Hysteresis in Perovskite Solar Cells", The Journal of Physical Chemistry Letters, vol. 5, no. 9, pp. 1511- 1515, 2014.

[16] N. Park, "Perovskite solar cells: an emerging photovoltaic technology", Materials Today, vol. 18, no. 2, pp. 65-72, 2015

[17] Tyagi, V.; Rahim, N.A.; Rahim, N.; Jeyraj, A.; Selvaraj, L. Progress in solar PV technology: Research and achievement. Renew. Sustain. Energy Rev. 2013, 20, 443–461.

[18] El-Adawi, M.K.; Al-Nuaim, I.A. The temperature functional dependence of VOC for a solar cell in relation to its efficiency new approach. Desalination 2007, 209, 91–96. [CrossRef]

[19] Singh, P.; Singh, S.N.; Lal, M.; Husain, M. Temperature dependence of I-V characteristics and performance parameters of silicon solar cell. Sol. Energy Mater. Sol. Cells 2008, 92, 1611–1616. [CrossRef]

[20] Siecker, J.; Kusakana, K.; Numbi, B.P. A review of solar photovoltaic systems cooling technologies. Renew. Sustain. Energy Rev. 2017, 79, 192–203. [CrossRef]

[21] Nijs, J.; Sivoththaman, S.; Szlufcik, J.; De Clercq, K.; Duerinckx, F.; Van Kerschaever, E.; Einhaus, R.; Poortmans, J.; Vermeulen, T.; Mertens, R. Overview of solar cell technologies and results on high efficiency multicrystalline silicon substrates. Sol. Energy Mater. Sol. Cells 1997, 48, 199–217. [CrossRef]

[22] Beg, R.A.; Sarker, M.R.I.; Parvez, R. An Experimental Investigation on Photovoltaic Power output through Single Axis Automatic controlled sun tracker. In Proceedings of the 4th BSME-ASME, Dhaka, Bangladesh, 27–29 December 2008.

[23] Zhao, Z.M.; Yuan, X.Y.; Guo, Y.; Xu, F.; Li, Z.G. Modelling and simulation of a two-axis tracking system. Proc. Inst. Mech. Eng. Part I J. Syst. Control Eng. 2010, 224, 125–137. [CrossRef]